Visit the Resource Center for more SIMULIA customer papers

Using the Failure Assessment Diagram Method with Fatigue Crack Growth to Determine Leak-before-Rupture

C. Tipple, and G. Thorwald

Quest Integrity Group, LLC

To evaluate if a crack may cause structural failure, the failure assessment diagram (FAD) method uses two ratios: brittle fracture and plastic collapse. The objective of this paper is to use Abaqus/Standard to compute elastic-plastic J-integral results along the crack front. These results are then used to calculate the plastic collapse crack reference stress, especially for cases when the reference stress solution is not available for a structural component. The FAD method is used in engineering best practice codes such as API 579-1/ASME FFS-1. A nozzle-cylindrical shell junction with a crack is used as an example to examine the details and common difficulties encountered in creating the crack model, obtaining the necessary elastic-plastic analysis convergence, and the additional calculation tasks to compute the reference stress from the J-integral values. In this example, the computed reference stress is used to obtain the plastic collapse ratio, Lr, and an elastic analysis is used to obtain the stress intensity to obtain the brittle fracture ratio, Kr. These ratios give the location of the evaluation point on the FAD to indicate structural failure or safety. Computing the FAD point is necessary to evaluate an existing crack found during inspection, or to evaluate the end-of-life critical crack size for a fatigue crack growth analysis. Engineers benefit from using Abaqus which computes the J-integral needed for the calculation of the reference stress and stress intensity for the specific crack location and the specific structural component geometry, avoiding the need to approximate the reference stress solution using a similar geometry.

Keywords: Brittle Fracture, Crack Mesh, Cyclic Load, Ductile Tearing, FAD, Fracture Assessment Diagram, Geometry Factor, Fatigue, Kr, Lr, Manway, Nominal Load, Nozzle, Plastic Collapse, Pressure Vessel, J-Integral, Reference Stress, Stress-Strain.

1. The failure assessment diagram method for assessing crack stability

To determine if a crack may cause a structural failure, the failure assessment diagram (FAD) method uses two ratios: brittle fracture and plastic collapse. The FAD method is described in the engineering best practice code API 579/ASME FFS-1 (API 2007), and in the fracture mechanics text book by T. L. Anderson (Anderson, 2005). The plastic collapse ratio is computed using the reference stress, which is computed using the J-integral results from the elastic-plastic Abaqus analysis. The brittle fracture ratio is computed from the crack front stress intensity, obtained by an elastic Abaqus analysis.

An example of the API 579 default FAD curve and crack evaluation points is shown in Figure 1. The axes of the FAD chart use the non-dimensional ratios Lr (plastic collapse ratio) on the x-axis, and Kr (brittle fracture ratio) on the y-axis. The example evaluation points inside the FAD curve

indicate acceptable cracks, and the evaluation points above the FAD curve are unacceptable cracks that indicate a predicted structural failure. An evaluation point on the FAD curve is a critical crack on the verge of failure, which can be useful to determine predicted critical crack sizes. When an analysis for a specific structural component and a stress-strain curve is available, a material specific FAD can be computed.

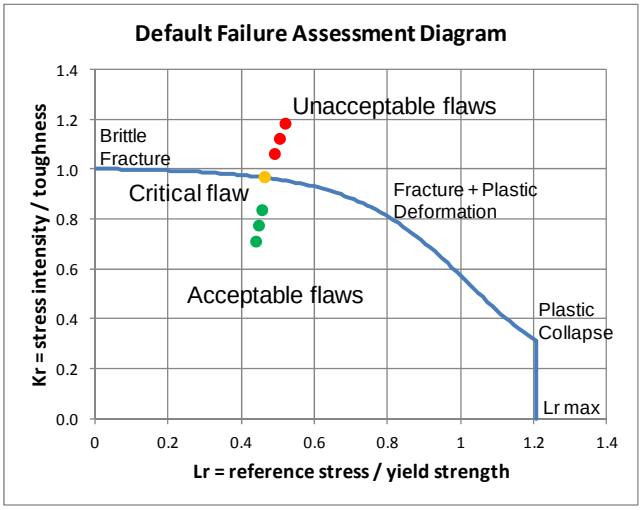

Figure 1. Example of the default FAD and crack evaluation points

To begin the reference stress calculation for the corner crack in the nozzle (Figure 6), the elastic J portion of the total elastic-plastic J-integral results is inferred by a curve-fit to the first few load increment values, using the J results at a specific crack front location. In general, the FAD calculations can be done for every crack front node position. For this example the position on the crack front where the maximum crack front J results at the final loading step is used.

Initially, when the internal pressure is low and the crack is still acting elastically, the maximum J values are located near the free surfaces of the crack front. As the pressure increases and the crack begins to exhibit elastic-plastic characteristics, the maximum J value generally occurs between the free surfaces within the ligament.

A quadratic curve fit is expected since J^2 is proportional to the stress intensity K, which is linear in the elastic range. Figure 2 shows a close-up of the first few J result analysis increments, and shows the quadratic curve fit using the first three data points (open circles). The elastic J trend is computed using the curve-fit (dashed line) and compared to the next several J increments (open square data points) to confirm that these results are in the expected elastic range and that the curve-fit is valid.

In a typical elastic-plastic analysis without a crack, the initial load increments can be large since equilibrium convergence is expected. However, for an elastic-plastic fracture analysis with a crack like this example, several small load increments are needed at the beginning of the analysis to ensure that there will be J results in the elastic range. The maximum load must be high enough to create yielding at the crack front, which is usually a much higher load value than the operating or design load.

The curve-fit is used to extrapolate and infer the elastic J trend for the higher load increments; Figure 3 shows the inferred elastic J trend (dashed line). The ratio of the total J to the elastic J at each analysis increment is needed in the reference stress and material specific FAD calculations.

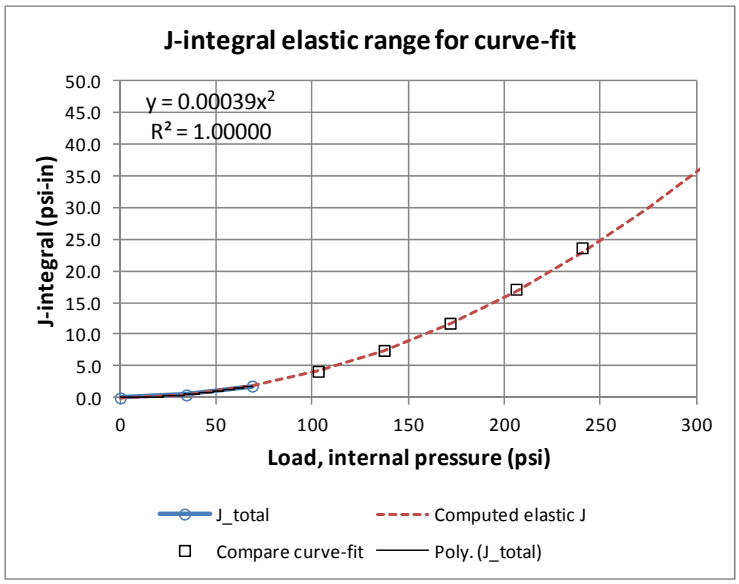

Figure 2: Quadratic curve-fit to the J results in the elastic range

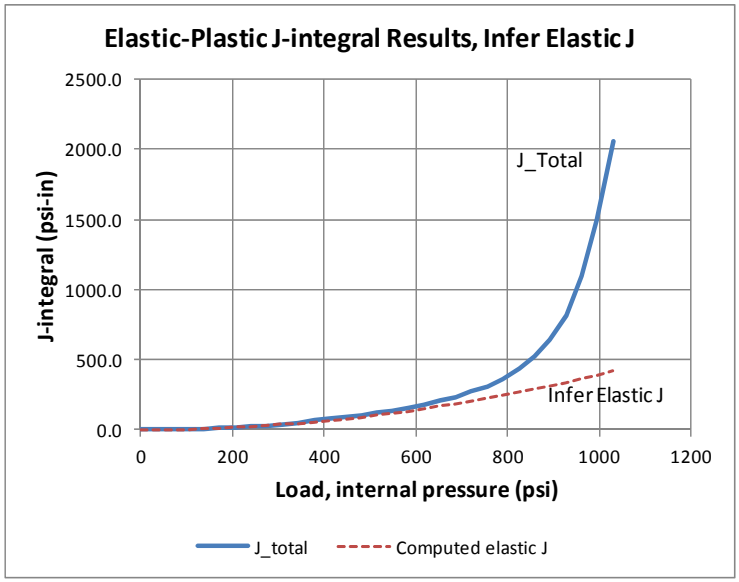

Figure 3: Infer the elastic J trend using the curve-fit

Next, the nominal load value is obtained by using the material specific FAD equation evaluated at Lr=1 (nominal plastic collapse). When the material specific FAD curve equation is evaluated at Lr=1, it takes this form given by (Anderson, 2005):

$$\left.\frac{J_{\text{total}}}{J_{\text{elastic}}}\right|_{Lr=1} = 1 + \frac{0.002E}{\sigma_{YS}} + 0.5\Big/\left(1 + \frac{0.002E}{\sigma_{YS}}\right) \quad (1)$$

The value of $J_{total}/J_{elastic}$ evaluated at Lr=1 is calculated using the modulus of elasticity, *E*, and the yield strength, σ_{YS}. The 0.002 value is the nominal 0.2% offset strain at yield. In this analysis the material values are: *E* = 30,000 ksi, and σ_{YS} = 45.8 ksi, giving the $J_{total}/J_{elastic}$ ratio value of 2.53.

The nominal load is obtained at the intersection of this ratio with the $J_{total}/J_{elastic}$ result curve; in Figure 4 the material specific ratio is shown by the horizontal dashed line, the J ratio result curve is the solid line, and the vertical dashed line shows the nominal load value at the intersection. Since the intersection point usually falls between data points, linear interpolation is usually needed to obtain the nominal load value. In this analysis, the nominal load is 934.35 psi. If the maximum applied load is not high enough, the J results will not be sufficiently large to get the intersection with the material specific J ratio value. If the maximum J is not large enough, then rerun the elastic-plastic analysis with a higher maximum load so that the J values will be large enough to evaluate the intersection point to obtain the nominal load.

The nominal load is obtained from the expected load at which Lr = 1, where nominal plastic collapse occurs. The nominal load is typically higher than the operating load. The nominal load is used to normalize the plastic collapse ratio values.

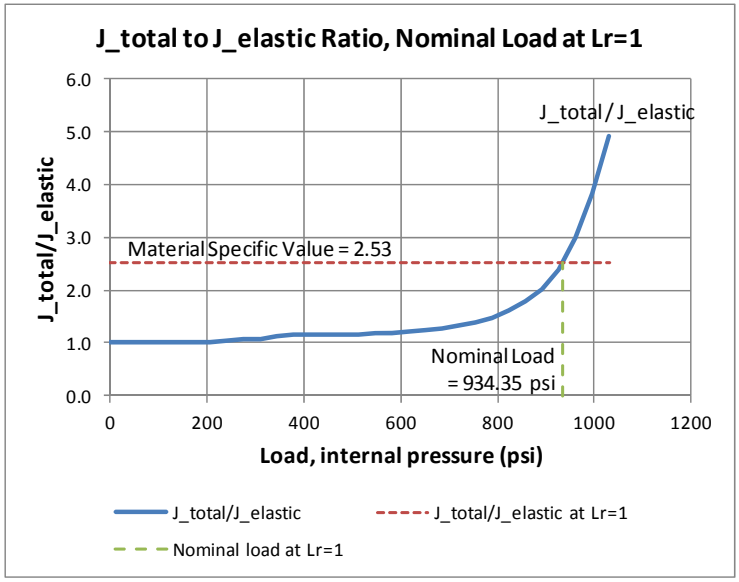

Figure 4: Finding the intersection of the J_total/J_elastic ratio and the result curve

The reference stress geometry factor, *F*, is defined as the ratio of the yield strength, σ_{YS}, to the nominal load obtained at Lr=1, $\sigma_{nominal|Lr=1}$ (Anderson, 2005).

(2) $$F = \frac{\sigma_{YS}}{\sigma_{\text{nominal}}|_{Lr=1}}$$

The nominal load value, $\sigma_{\text{nominal}}|_{Lr=1}$, obtained from the intersection point in Figure 4, gives the reference stress that satisfies the material specific FAD equation at Lr=1, and is used to normalize the FAD Lr axis values. In this analysis the reference stress geometry factor *F* is 46.97.

Now the reference stress and Lr values can be computed for each analysis increment to obtain the analysis specific and material specific FAD Lr values. The reference stress, σ_{ref}, at each load increment is given by:

(3) $$\sigma_{\text{ref}} = F\sigma_i$$

Where *F* is the geometry factor and σ_i is the load value at each load increment *i*. The FAD curve Lr values are computed at each load increment using the equation:

(4) $$Lr = \frac{\sigma_{\text{ref}}}{\sigma_{YS}} = \frac{F\sigma_{\text{i}}}{\sigma_{YS}}$$

Where σ_i is the load value at each load increment *i*, and σ_{YS} is the yield strength. The FAD curve Kr values at each load increment are given by the equation using the $J_{elastic}$ / J_{total} ratio:

(5) $$Kr = \sqrt{\frac{J_{\text{elastic}}}{J_{\text{total}}}}$$

Where J_{total} are the elastic-plastic analysis J-integral results, and the $J_{elastic}$ values were obtained from the curve-fit to the first few result increments in the elastic range. Figure 5 compares the default FAD curve to the computed FAD curve specific to this analysis and material data. The two curves are similar, and using the default FAD curve is usually sufficient to evaluate a crack, but the computed FAD curve can provide a better representation of the effect of a particular material's stress-strain curve and the particular structural component geometry.

The maximum Lr cutoff value should also be applied to the computed FAD curve to determine the plastic collapse limit (API 2007). In many cases the Lr cutoff value is given by the ratio:

(6) $$Lr_{\text{max}} = \frac{\sigma_{YS}+\sigma_{TS}}{\sigma_{YS}}$$

Where σ_{YS} is the yield strength and σ_{TS} is the tensile strength.

The crack FAD evaluation point is computed using the stress intensity from the elastic analysis and the reference stress at the given load. The Lr value is computed using the same Lr equation:

(7) $$Lr = \frac{\sigma_{\text{ref}}}{\sigma_{YS}}$$

But in this instance of the equation σ_{ref} is the reference stress at the given evaluation load, usually the design load or the operating load, and σ_{YS} is the yield strength. The Kr value is computed using the elastic stress intensity, K, and the material toughness K_{mat} with this equation:

(8) $$Kr = \frac{K}{K_{\text{mat}}}$$

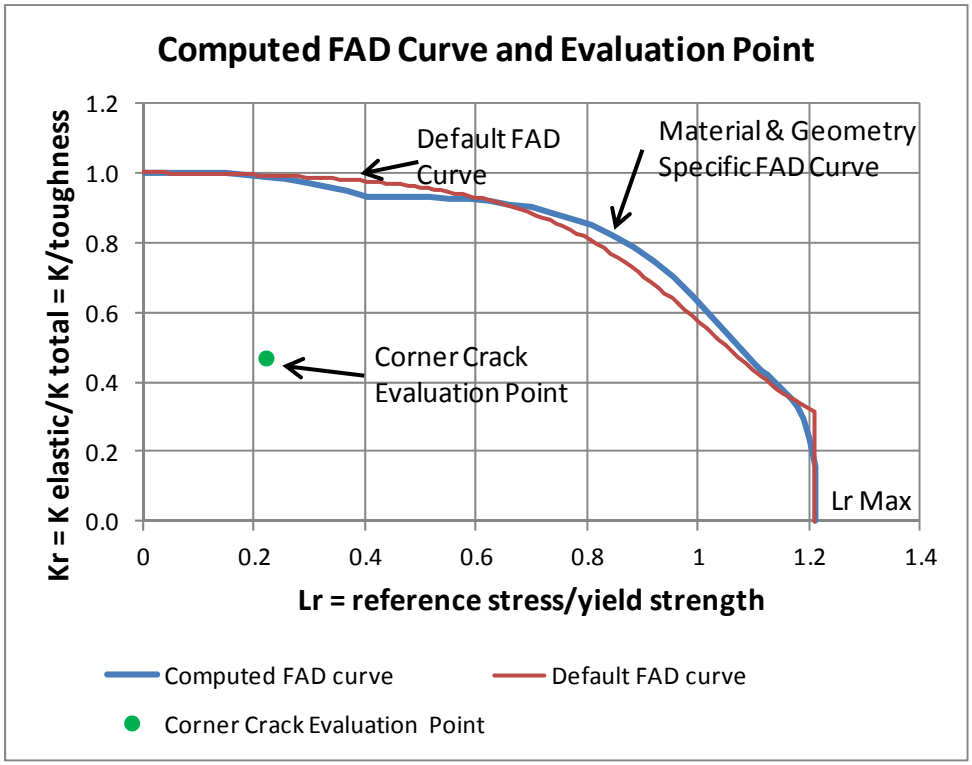

Figure 5: Comparing the material-specific FAD and the default FAD curves

Figure 5 shows the corner crack evaluation point on the FAD chart. In this analysis Lr is 0.22, and Kr is 0.47, which is inside the FAD curve and is considered an acceptable size crack.

This nozzle component has cyclic loading, and the FAD evaluation point can be updated as the crack grows to determine the end of life when the evaluation point reaches the FAD curve indicating a critical crack size for failure. Using a combination of an elastic-plastic analysis to obtain J values and an elastic analysis to obtain the stress intensity K, a crack can be evaluated for fracture in a specific structural component. This is especially useful when a handbook fracture solution is not available, such as the nozzle to shell structure that is examined here.

2. Crack growth analysis to establish leak-before-rupture

Using the FAD method, a leak-before-rupture assessment is performed for a horizontally oriented carbon dioxide storage vessel. Located on the top of the vessel is a set-in type 300# ANSI manway. This manway is reinforced with an externally welded reinforcing pad. The reinforcing pad does not directly adhere to the shell except at the full penetration weld at the manway, and at the fillet weld on the outer circumference of the reinforcing pad to the vessel shell.

2.1 Probable crack location

A three-dimensional, linear elastic, quarter-symmetric model is used to represent the geometry of the manway-shell junction, shown in Figure 6. This geometry contains 8,565 quadratic hexahedral elements (Type C3D20R) and 42,075 nodes.

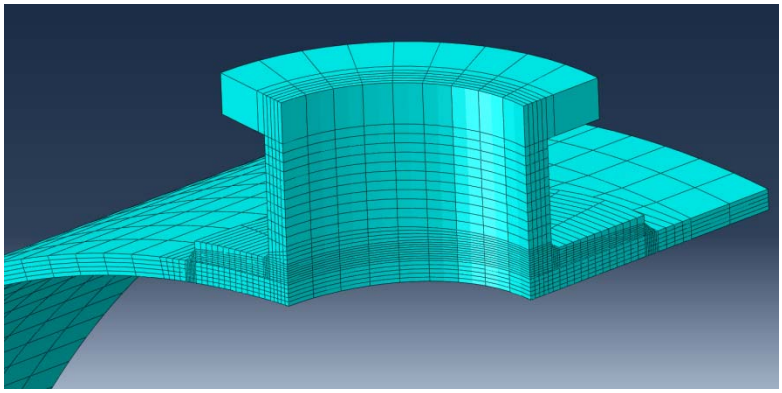

Figure 6: Quarter symmetric manway-to-shell model

The material properties are representative of a structural steel alloy, with the modulus of elasticity of 30,000 ksi and the Poisson's ratio of 0.3 (Norton, 2006). Under operating conditions, this component does not yield.

The internal surface of the vessel, including the shell and manway internal surfaces, is subject to an internal pressure of 206 psi (the operating pressure of the vessel). Corresponding proportional tensile axial pressure thrusts are uniformly applied to the end of the vessel and to the manway flange.

A symmetric boundary condition is applied on each of the two perpendicular planar faces of the manway and shell. A vertical constraint is applied on a single node to adequately constrain the model.

The intended purpose of this model is to identify the direction and magnitude of the maximum tensile principal stress, which gives the location for potential crack initiation and the expected direction of propagation. The maximum tensile principal stress is found to be on the internal surface at the junction of the vessel shell and the manway, shown in Figure 7. Furthermore, the maximum principal stress is oriented in the vessel hoop direction, shown in Figure 8.

It is likely that a potential crack initiates at the location with the highest maximum principal stress, and that the crack propagates perpendicularly to the direction of that maximum principal stress. It is expected that a longitudinal corner crack could initiate at the inside corner of the shell and manway and propagate in the axial direction of the vessel.

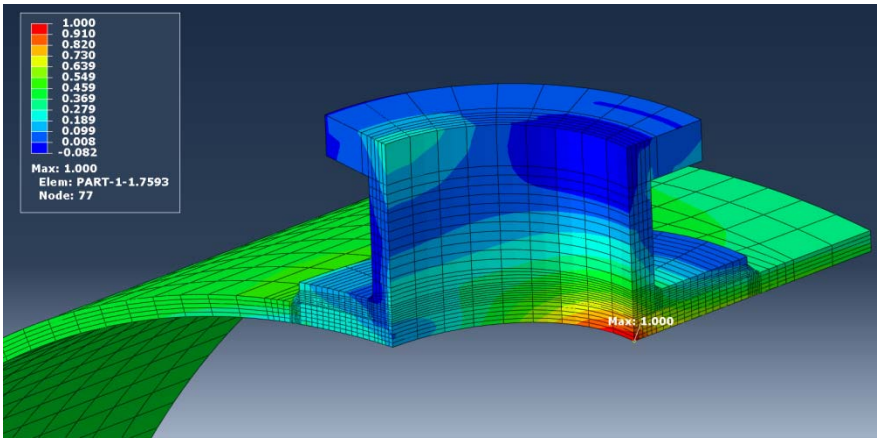

Figure 7: Magnitude of maximum principal stress, normalized to the maximum value

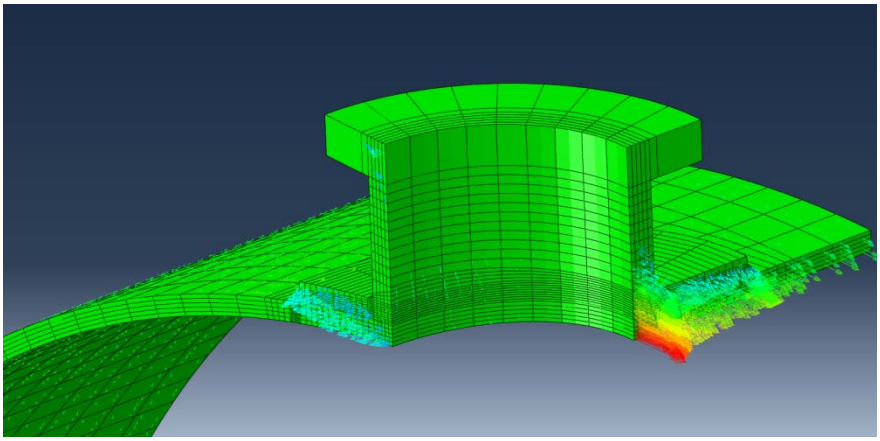

Figure 8: Direction of maximum principal stress

2.2 Global Stress Profile Including Crack

A crack mesh was incorporated into the shell-manway geometry using tied contact, and the stress pattern at the tied contact boundaries will be compared to the uncracked model. The crack was modeled at the high stress location (discussed previously) as a semi-circular corner crack, shown in Figure 9 (FEACrack™, 2010).

The crack-inclusive model has the same material properties boundary conditions as described previously. The loading conditions and symmetry constraints are also the same with the internal pressure applied to the crack face. Global maximum principal stresses are shown in Figure 10 and a close-up of the maximum principal stress is shown in Figure 11.

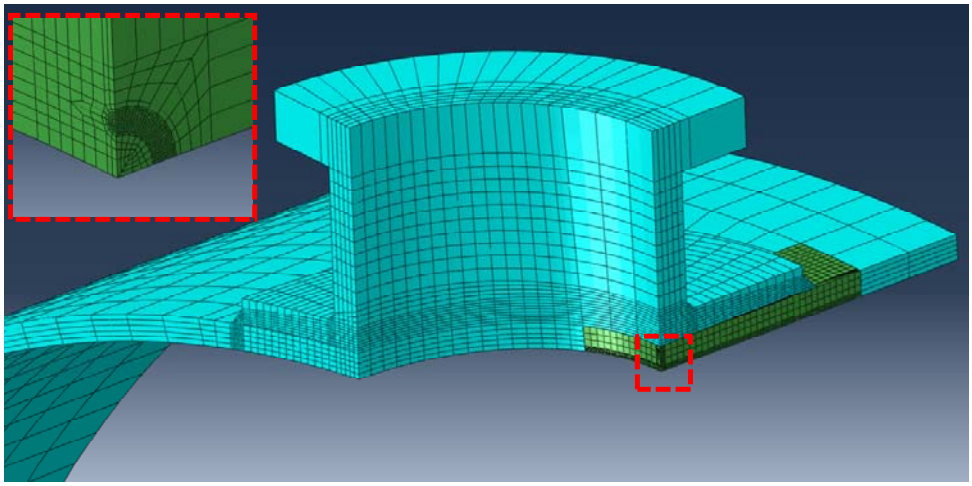

Figure 9: Shell-manway model incorporating crack mesh via tied contact (crack mesh shown in dark green)

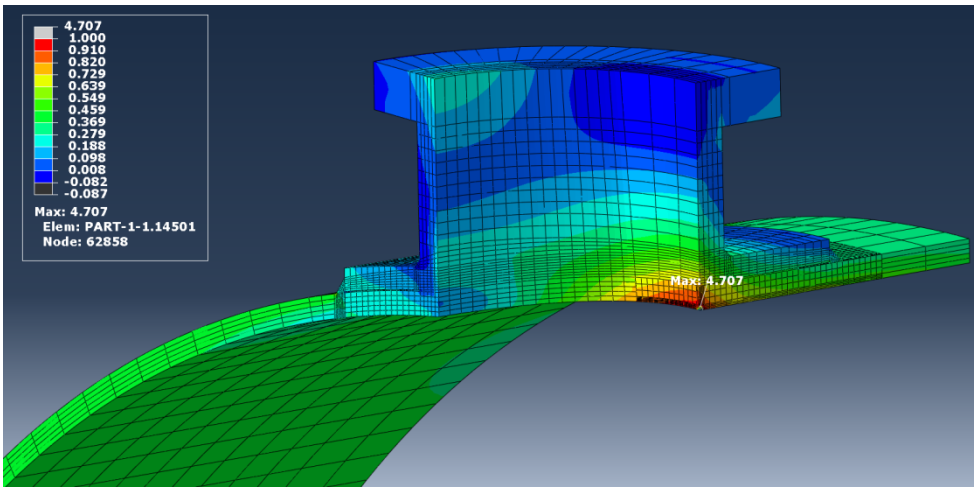

Figure 10: Magnitude of the maximum principal stress global results, normalized to the un-cracked model's maximum value of the maximum principal stress

It can be observed that the maximum principal stress contours in both Figure 7 and Figure 10 (representative of an un-cracked geometry and a cracked geometry, respectively) are almost identical at the tied boundary between the crack mesh and the surrounding model. As a result, the introduction of a small crack has only a localized stress influence near the crack front.

The global stress results at the tied boundary remain unchanged, provided that the crack's dimensions are small compared to the host crack mesh. Therefore, as the crack grows due to cyclic pressure loading, a submodel can be used for the crack growth analysis.

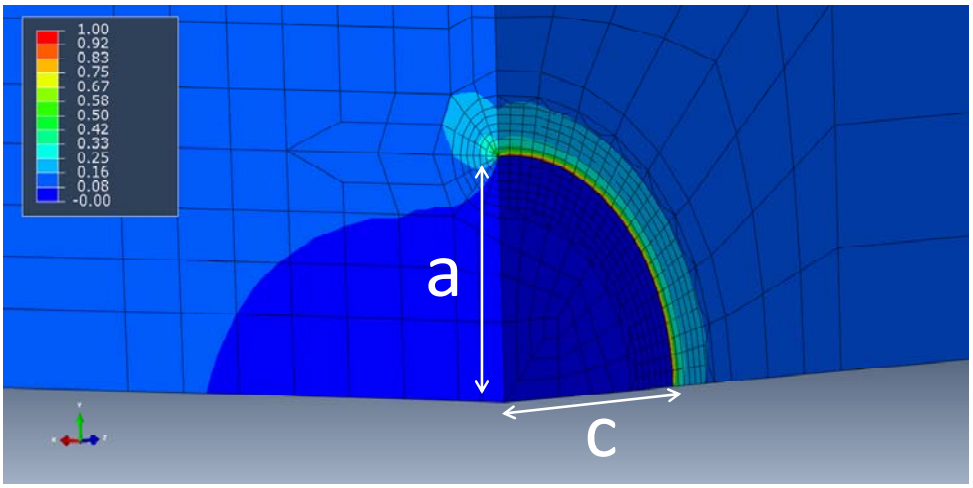

Figure 11: Magnitude of the maximum principal stress near-crack results, normalized to the model's maximum value of the maximum principal stress

2.3 Fatigue Crack Growth

Crack growth is computed using the Paris equation, using a coefficient and an exponent recommended for austenitic steel in a non-aggressive environment, of $C = 8.61 \times 10^{-19}$ and $m = 3.0$, respectively (for stress intensity in psi√in and crack growth in in/cycle) (API 579, 2007).

$$\frac{da}{dN} = C(\Delta K)^m \tag{9}$$

The fatigue threshold stress intensity is assumed to be zero, therefore every cycle contributes to crack propagation. The internal pressure of the vessel cycles from zero to the design pressure.

An elastic finite element model is used to compute the crack front stress intensity at the peak magnitude of the cyclic load and at the operating pressure for each increment of crack growth.

An example of the crack sub-model is shown by the dark green mesh in Figure 7. Crack growth is modeled using an appropriate number of crack growth iterations to sufficiently converge on a solution.

The initial sub-model included a corner crack of dimensions a=c=0.50 inch. Using the stress intensity along the crack front, the Paris equation is solved, at each iteration, for the number of cycles and the crack length for a specified incremental crack depth change. Starting at a depth of a=0.50 inch, the incremental crack depth is increased by 0.05 inch until the crack depth reached 1.00 inch. This is shown in addition to the crack driving stress contours in Figure 12. Note that the corner crack aspect ratio changes from semi-circular to a longer elliptical profile during the crack growth.

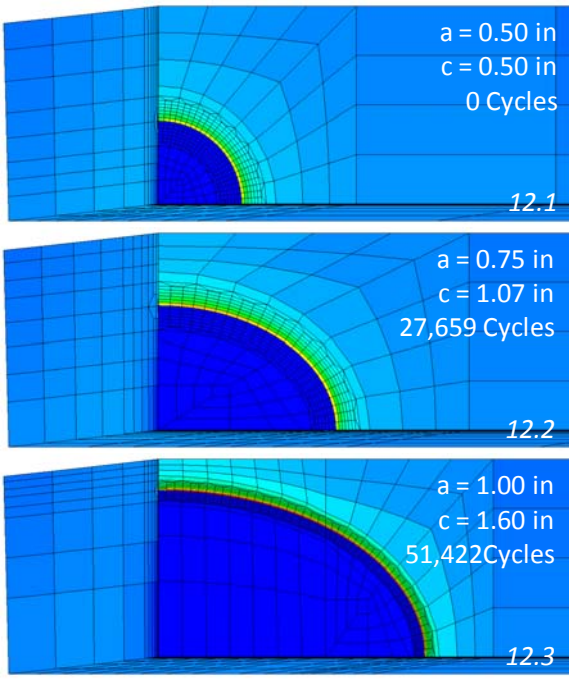

Figure 12: Incremental crack growth, shown with the corresponding crack depth "a" crack length "c" and number of cycles

2.4 Recharacterization of surface crack

According to published literature, once the crack depth reaches 80% of the total thickness, the crack can be recharacterized as a surface breaking crack (API 579, 2007). Once the crack depth reaches 0.95 inch (or 80% of the total ligament thickness) during the fatigue crack growth, the resulting crack length must be known to recharacterize the corner crack.

To recharacterize the crack, a second order polynomial interpolation shown in Figure 13 was used to identify the number of cycles for the crack to reach 80% depth, which is 46,279 cycles.

To identify the crack length at this number of cycles, a second order polynomial interpolation, shown in Figure 14, was used to identify the crack length of 1.49 inches at that number of cycles.

Now, the crack can be recharacterized as a surface breaking crack according to the following expression (API, 2007).

(10) $$c_t = c_s + (t - a_s)$$

Where c_t is the through thickness crack length, c_s is the surface flaw length, a_s is the surface flaw depth, and t is the uncracked wall thickness.

Using equation 10 to recharacterize the crack, the 80% through thickness crack can be recharacterized as a through-wall crack of length 1.73 inches.

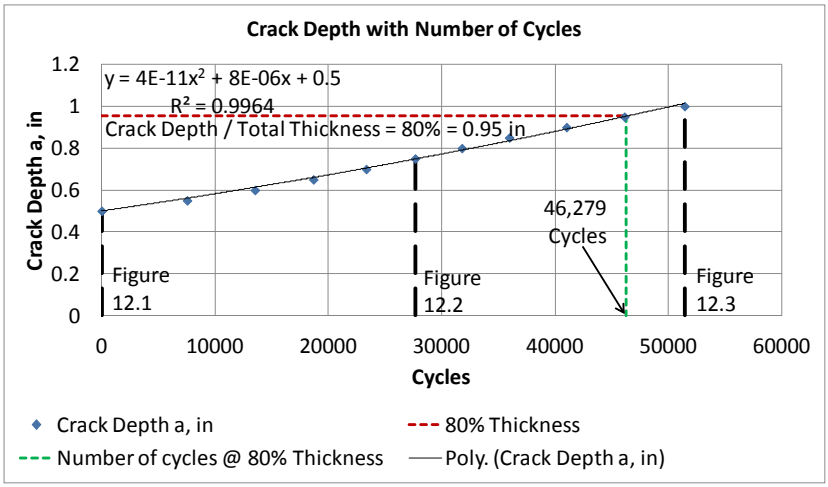

Figure 13: Crack depth with number of cycles

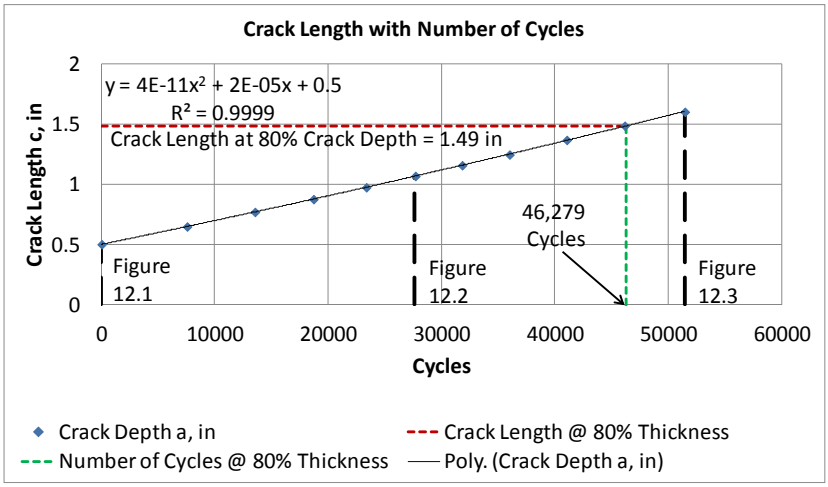

Figure 14: Crack length with number of cycles

The vertical dashed lines shown in Figure 13 and Figure 14 correspond to the crack geometries shown in Figure 12.

2.5 Final assessment of recharacterized through-wall crack

The final through-wall crack (dimension c = 1.73 inches) is assessed using the failure assessment diagram method, discussed in Section 1. The only difference between this assessment and the assessment shown in Section 1 is that the crack geometry is now a through-wall edge crack rather than a semi-elliptical corner crack. A picture of the through-wall surface crack sub-model mesh is shown in Figure 15.

The elastic-plastic properties used to find the elastic J values along the crack front are shown in Figure 16.

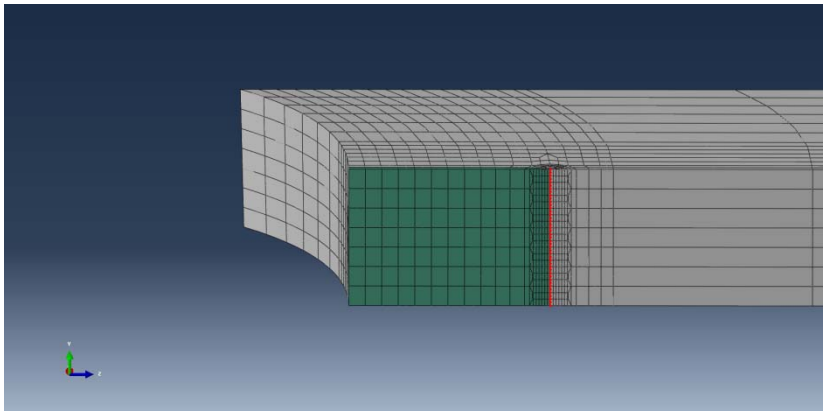

Figure 15: Through-wall crack mesh (green face represents crack face and red points represent crack front nodes)

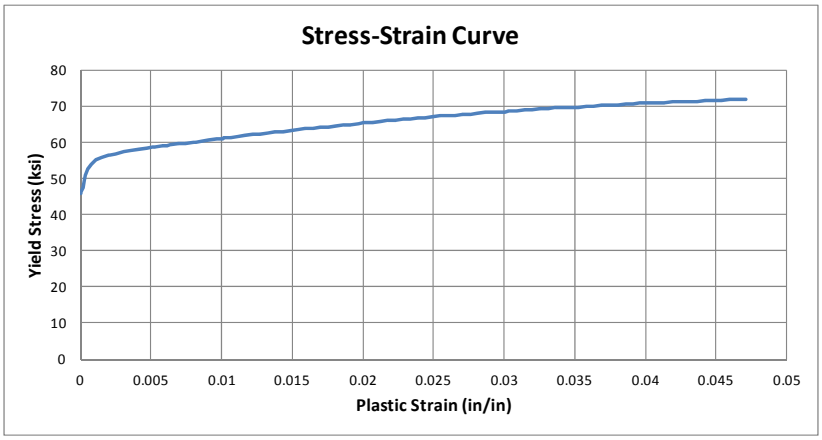

Figure 16: True tress-plastic strain curve for elastic-plastic sub-models

Finding the intersection between the J_total / J_elastic constant material specific value (2.53) and the J_total / J_elastic curve computed from the results of the finite element models, the reference stress identifies the nominal load, which will then be used to find the geometry factor *F*, shown in Figure 17. The resultant geometry factor, *F*, is 50.63.

The FAD can then be evaluated, and the assessment point for the through-wall crack in the vessel shell can be updated to reflect the results of a through-wall crack under operating loads. Shown in Figure 18, the recharacterized through-wall crack evaluation point still lies below the FAD curve, therefore the through-wall crack is not at risk for sudden rupture. Finally, the through-wall crack front in the vessel shell is long enough to be below the repad. There gap between the repad and the vessel shell that is exposed to the atmosphere via small pressure-relieving holes. If the

through-wall crack forms, there would be a leak path from the inside of the vessel, through the crack in the shell, to the exterior, so that a leak could be observed.

.

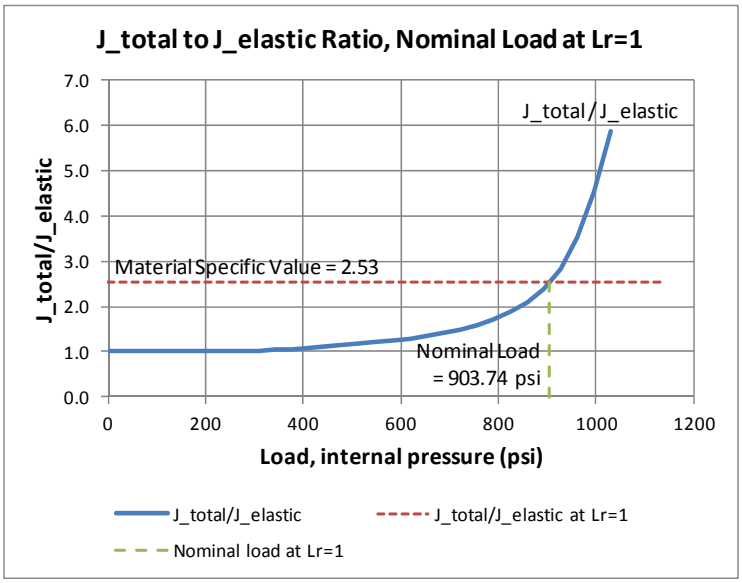

Figure 17: Finding the intersection of the J_total/J_elastic ratio and the result curve for the through-wall crack

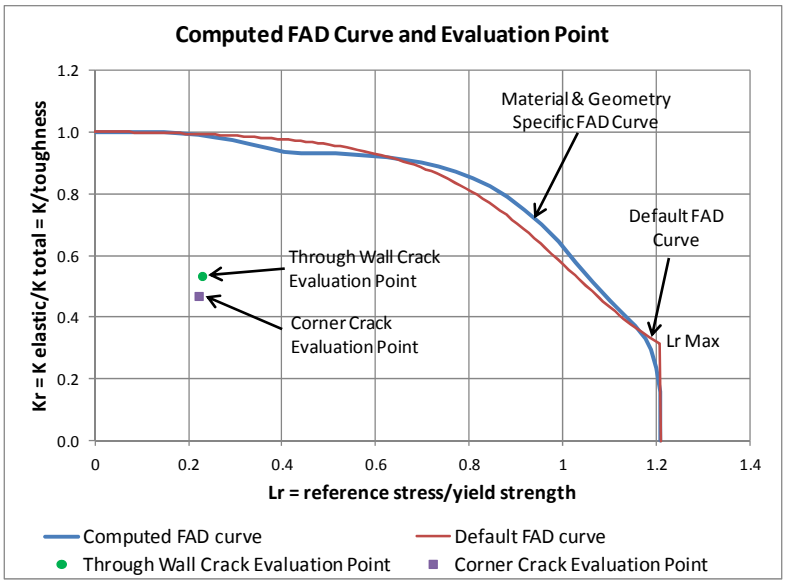

Figure 18: Comparison of the material-specific FAD and the default FAD curves and plot assessment points for through-wall and corner cracks

When the corner crack grows to a through-wall crack in the shell, there would also be a through-wall crack formed in the nozzle. The nozzle through-wall crack can be evaluated in the same way that the shell through wall crack was evaluated. The through wall crack in the shell was chosen for evaluation because the crack length was growing faster than the crack depth, so it was anticipated that the crack length would be the larger crack dimension, and is likely to be the worst case.

3. Concluding Remarks

The J integral is calculated along the crack front of an internally-breaking corner crack at the junction between a vessel's shell and a manway. Using both elastic and elastic-plastic J integral results, crack stability is identified using the FAD method using the brittle fracture ratio, Kr, and the plastic collapse ratio, Lr.

The crack's dimensions are then calculated, resulting from cyclic fatigue loading, based on the Paris equation. The crack tended to propagate at a faster rate in the length direction (c) than the depth direction (a). After propagation, the corner crack is then recharacterized as a through-wall crack, and evaluated using the FAD method. The through-wall crack is sufficiently small, that its assessment point lies under the FAD curve, and is not a risk for sudden rupture. Finally, provided that the contents of the vessel leaking from the crack can be detected, and adequate detection instrumentation is operating, then the vessel will likely leak before rupture.

4. References

1. Anderson, T. L., "Fracture Mechanics, Fundamentals and Applications", 3rd ed., 2005, CRC Press, Taylor & Francis Group, section 9.4, pp. 410-423.
2. Anderson, equation 9.69, p. 418.
3. Anderson, equation 9.71, p. 418.
4. API 579-1/ASME FFS-1, June 5, 2007 "Fitness-For-Service", The American Society of Mechanical Engineers and the American Petroleum Institute, Paragraph F.5.3.2.a.
5. API 579, Figure 9.20, Part 9.
6. API 579, Equation 9.29, Part 9.
7. FEACrack, Version 3.2.14, 2010, Quest Integrity Group, Boulder, CO, http://www.questintegrity.com/products/feacrack-3D-crack-mesh-software/.
8. Robert L. Norton "Machine Design an Integrate Approach", 3rd ed., 2006 Worcester Polytechnic Institute, Worcester, Massachusetts, Page 944, Table C1

Visit the Resource Center for more SIMULIA customer papers